Observation of $2p^3$ states in the electron-ionization efficiency curve of helium between 58 and 59 eV

R. N. Gosselin* and P. Marmet
Herzberg Institute of Astrophysics, National Research Council of Canada, Ottawa, Canada K1A 0R6
(Received 27 June 1989)

High-resolution ionization efficiency curves using electron impact (58–59 eV) on helium are presented. Two previously unknown structures are clearly seen in the spectra at 58.415±0.005 and 58.48±0.02 eV in addition to the large $(He^*)^-2s2p^2(^2D)$ negative-ion resonance. The line-shape parameters for the ^2D state obtained by fitting the data to theoretical line profiles are $E_R = 58.283 \pm 0.003$ eV, $\Gamma = 59 \pm 4$ meV, and $Q = -0.70 \pm 0.04$. The two new structures are tentatively assigned to the $(He^*)^-2p^3$ electron configuration.

I. INTRODUCTION

High-resolution data showing total ionization cross sections of low energy, monoenergetic [full width at half maximum (FWHM) of about 20 meV] electrons on He atoms are reported. Both negative-ion and neutral discrete states interact with the ionization continuum to produce perturbations (i.e., structure) in the ionization efficiency curve. However, in the narrow energy range between 58 and 59 eV, the only structure previously reported in the ionization efficiency curve was that due to the large negative-ion resonance $2s2p^2(^2D)$. A simple visual inspection of our data (see Figs. 1 and 2) clearly shows the presence of two other structures.

None of the data were taken with the intention of fitting of theoretical line profiles, but simply to confirm the existence and the position of the new structures. As a result the range of energy used was not ideally suited to the requirements of the fitting procedure. These requirements are discussed later in the paper. However, fits of the data to theoretical profiles do reveal that there are actually a total of four distinct structures in this energy range. The additional feature detected through the fit has parameters corresponding to the neutral state $2s2p(^3P^\circ)$.

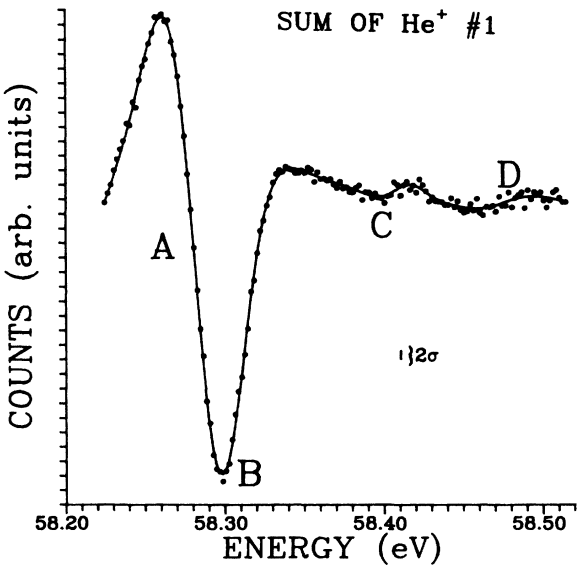

FIG. 1. Electron-ionization efficiency curve for helium for the sum of three data sets (1A,1B,1C) taken at 1 meV/channel (2 meV/channel plotted). The solid line is the best fit (four-profile) theoretical curve (see text). The number of counts per channel is about 900×10^6.

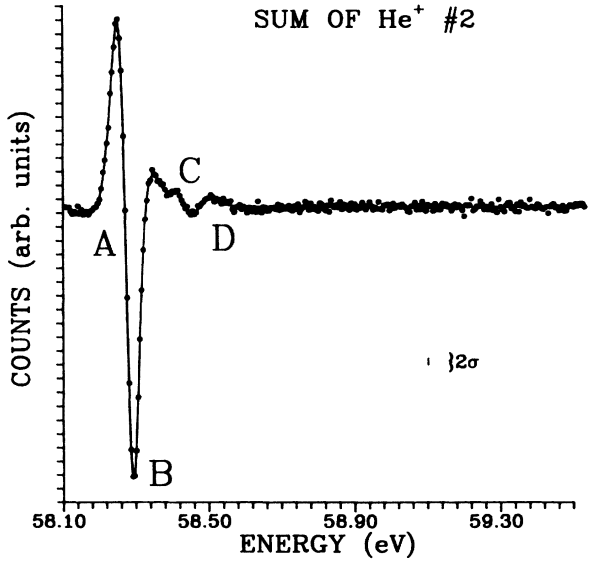

FIG. 2. Electron-ionization efficiency curve for helium for the sum of three data sets (2A,2B,2C) taken at 5 meV/channel. The solid line is the best fit (four-profile) theoretical curve (see text) with the same parameters (within the estimated error) as that of Fig. 1. The number of counts per channel is about 450×10^6.

II. EXPERIMENT

The very narrow energy distribution of the electron beam was obtained using two cylindrical energy selectors in series (for details of the experimental arrangement, see Ref. 1). This beam (~ 1 nA) crossed a helium beam (molecular flow) directed towards a large aperture, electric-quadrupole mass spectrometer. The number of helium ions arriving at the exit of the spectrometer was counted by means of an electron multiplier tube. Typical ion count rates at an incident energy of 58 eV were between 100 000 and 200 000 counts/s. The background counting rate (measured with either no electron beam or the mass spectrometer tuned off the He peak) was between one and two counts per minute.

The ion count as a function of electron energy was measured by applying a constant base voltage in series with an offset voltage which increased linearly with time (i.e., a ramp of 1 V/s). The offset voltage was swept from zero to some preset value, each sweep taking less than 0.8 s. Each data set is the sum of over 100 000 successive sweeps, thus minimizing systematic errors due to fluctuations in various experimental parameters (e.g., electron current and helium flux). However, in order to avoid broadening the structures due to the inevitable small drift in contact potential within the electron source, accumulation was halted every 24 h in order to compensate for this drift. The position of the minimum of the negative-ion resonance was used to determine how much of a shift was necessary. In all cases the shift was no more than 1 meV per day.

Absolute calibration of the energy scale was accomplished by measuring the position of the first ionization threshold of helium at 24.5876 eV. The position of the threshold on our scale was consistently determined to within 1 meV. This difference (i.e., an effective source contact potential, typically about 50 meV) was then used to calibrate the point of steepest descent of the large negative-ion resonance in the region of interest. A small correction of about 4.6 meV due to the maximum energy loss allowed by conservation of momentum was also taken into account.

III. ANALYSIS OF DATA

The curves shown in each of Figs. 1 and 2 are the sum of three data sets (i.e., a total of six independent data sets). The slowly varying background has been greatly attenuated by filtering out the low-frequency components of the spectrum. In order to show the spectral features more clearly a slightly different filter was used for the two cases shown. This produces a small alteration in the apparent shapes of the structures and only has a small effect on the results of the fitting procedure since the fitting function(s) are also subjected to the same filtering as the experimental data to which they are compared. One of two possible line profiles was considered in attempting to fit a particular structure; one corresponding to a negative-ion state and the other to a neutral state.

The cross section for the production of a negative-ion resonance (i.e., absorption of the incident electron) can be approximated by one of the family of curves (Fano profiles[2])

$$\sigma(\varepsilon)=A\frac{(Q+\varepsilon)^2}{1+\varepsilon^2}+B \quad \text{where } \varepsilon=(E-E_R)/(\Gamma/2) . \tag{1}$$

The constant term B is removed completely by the filtering process. The width of the structure corresponds to the lifetime of the state ($\Gamma=\hbar/\tau$) and E_R is the energy of the state. The effect of varying the line-shape parameter Q is illustrated in Fig. 3. The structure produced in the ionization efficiency curve due to the presence of a neutral state is approximately given by the integral of Eq. (1) from the ionization threshold to the energy of the incident electron. This is described by a second family of curves[3]

$$\sigma(\varepsilon)=A[(Q^2-1)\tan^{-1}(\varepsilon)+Q\ln(\xi^2+1)] . \tag{2}$$

Constant and linear terms have been dropped since they are both completely removed by the filtering process. This family of curves is shown in Fig. 4. After this high-pass filtering, these integrated profiles look much like unfiltered Fano profiles. This is a source of some uncertainty in determining the correct fitting function due to the presence of noise (Poisson statistics) and due to the fact that the line profiles are perturbations of the ionization continuum. Since this continuum varies slowly as a function of electron energy, this variation can affect the line profiles.

The fitting procedure also allowed for the convolution of a symmetric, approximately Gaussian, electron energy distribution with the theoretical profile(s). The actual distribution is likely to be slightly asymmetric. This is another source of uncertainty in the fit. In practice the fits are not very sensitive to small variations in the

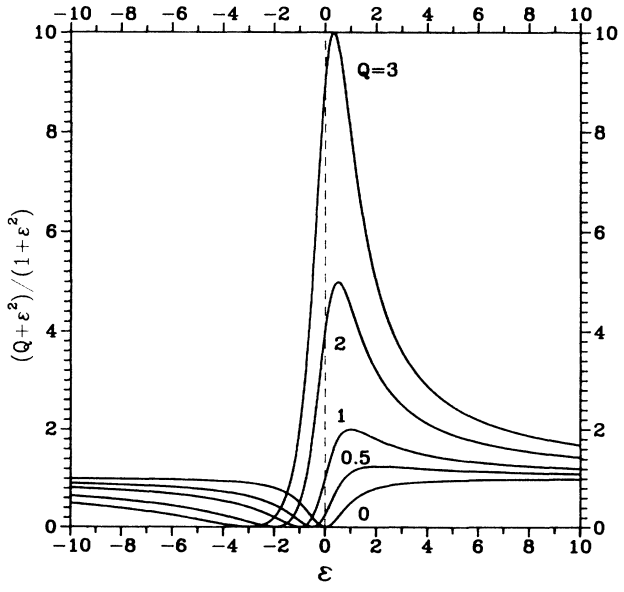

FIG. 3. Fano profiles for several values of the line-shape factor Q. Reverse the abscissa for negative values of Q.

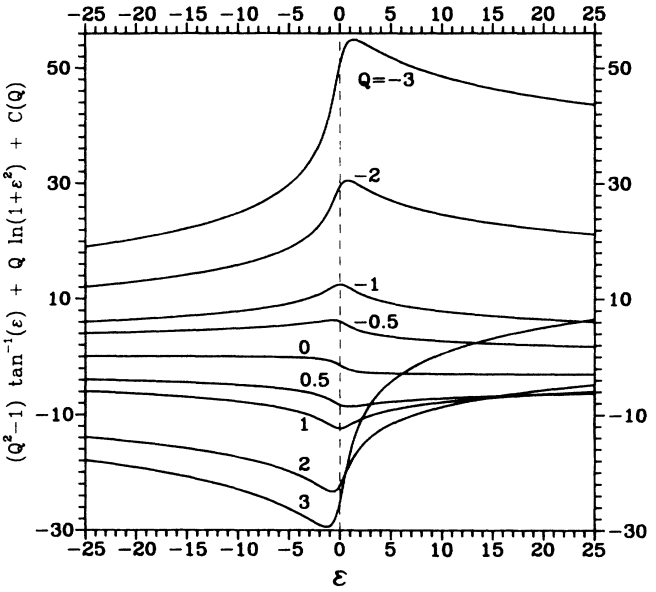

FIG. 4. Integral of the Fano profiles for several values of the line-shape parameter Q. An arbitrary constant $C(Q)$ has been added to the curves shown in the figure.

FWHM used. The best fits are obtained with a FWHM of 21 meV for the individual data sets (2A,2B,2C). The summed data sets have an increased effective width (FWHM ~ 25 meV) since one can only align the data sets to within one channel. This effective width is a reasonable value given the operating conditions of the electron selector. However, since this distribution is only an approximation, one might expect larger uncertainties in the parameters when fitting a structure whose width is smaller than 20 meV.

The fitting of the data would be better if more data points had been taken on the low-energy side of the first resonance. The first data points in sets 1A,1B,1C are more than halfway up the peak (before removal of low-frequency components) of the large resonance. As a result, they are not ideally suited for fitting to theoretical profiles, although the results of the fits are consistent with sets 2A,2B,2C. The best results (i.e., lowest values of the reduced χ^2) are obtained from data sets 2B and 2C which are the only sets taken with the signal at the background level on the low-energy side of the large resonance. The data presented here represent over two months of continuous accumulation and the gathering of similar data over a wider energy range will require a correspondingly longer acquisition time.

IV. DISCUSSION OF RESULTS AND CONCLUSIONS

The main result of interest is the observation of the two new structures in the spectrum. This should be useful to theoreticians as one of the simplest examples of a three-electron, triply excited atomic system. It is useful to try to explain the observed spectrum in the simplest possible terms. In particular, it is important to see how well the results can be interpreted when one does not include any post-collision-interaction (PCI) effects and assume a simple superposition of negative-ion and neutral states represented by the Fano and integrated Fano profiles. As indicated below, this simple analysis does give a good quantitative agreement with the observed spectrum. The simplest interpretation of these results is that the new structures are negative-ion states whose parent state is

TABLE I. Sample fits of three of the data sets using a high-pass filter whose 50% cutoff point is about 265 meV (53 channels). (a) One Fano profile(F) with upper energy limit of 58.28 eV (structure A alone). (b) One Fano profile and one integrated profile (IF) with upper energy limit of 58.33 eV (structure A and B together). (c) Parameters for the $2s2p(^3P^\circ)$ state from other experimental results. Numbers in parentheses denote the estimated error in the last digit. Numbers in square brackets are probabilities that the χ^2 is greater than the value obtained.

DS	*E* (eV)	Γ (meV)	*Q*	χ^2 [Probability (%)]
		(a)		
2A(F)	58.281(2)	58(2)	−0.74(4)	1.35[16]
2B(F)	58.281(2)	55(2)	−0.69(3)	0.89[69]
2C(F)	58.279(2)	59(2)	−0.75(3)	1.03[42]
		(b)		
2A(F)	58.282(2)	60(2)	−0.76(4)	
2A(1F)	58.311(3)	8(5)	4(1)	1.40[10]
2B(F)	58.284(2)	61(2)	−0.80(4)	
2B(1F)	58.309(3)	8(3)	2.9(7)	0.90[65]
3B(F)	58.282(2)	63(2)	−0.83(4)	
3B(1F)	58.307(3)	6(3)	2.8(6)	1.16[22]
		(c)		
	58.312[a]	9.3±0.7[b]		
		<7.12±0.12[c]		

[a]Reference 5.
[b]Reference 6.
[c]Reference 7.

TABLE II. Summary of the results obtained by fitting spectra to theoretical profiles. The electron affinity (EA) of the parent state for the observed negative-ion states is given in the last column. The numbers in parenthesis represent the estimated error in the last digit(s).

E_R (eV)	Γ (meV)	Q	State	EA (eV)
58.283(3)	59(4)	−0.70(4)	$2s2p^2(^2D)$	0.026(5)
58.309(3)	8(3)	4(2)	$2s2p(^3P^\circ)$	Not available
58.415(5)	<2	7(3)	$2p^2(^3P)2P(^4S^\circ)$	1.259(5)
58.48(2)	70(20)	1.0(5)	$2p^2(^1D)2p(^2D^\circ)$	1.42(2)

the next highest neutral state ($2p^2$). The absence of PCI effects in our data, as compared with the results of van der Burgt, van Eck, and Heideman[4] is likely because we do not measure one excitation channel at a time. We measure the total ionization cross section. The sum of PCI effects over an infinite number of structures with differing frequency and phase would greatly attenuate these structures in the integrated cross section.

A. The $2s2p^2(^2D)$ and $2s2p(^3P^\circ)$ profiles

A good fit of the largest feature to a Fano profile is obtained by restricting the energy range of the fit to below 58.28 eV. Such a restriction is necessary because above that energy the perturbation produced by the $2s2p(^3P)$ state is too strong to fit the curve to a single profile. For example, the three data sets of Fig. 2 were analyzed using the same filtering function and upper energy limit. The resulting parameters are shown in Table I, along with the reduced χ^2 and the probability that the χ^2 would be as large as that observed. The quoted errors represent the estimated errors from the least-squares fit as well as the uncertainty of 1 meV in the calibration of the energy scale. These error estimates must be interpreted as indicating the consistency of the fit between data sets rather than an actual estimated uncertainty in the resonance energy. There is additional uncertainty due to the effects of the partially overlapping and/or unresolved structures (including possible residual PCI effects) and the approximate nature of the fitting function. Although the E_R obtained from the fit does increase systematically with decreasing filter bandwidth, the variation results in only a fraction of a channel change (~ 1.2 meV) for both the energy and width of the state. These small variations are included in the final estimated error for each of the parameters.

The effect of an overlapping structure on the large resonance can be seen extending the fitting region by ten channels to 58.33 meV, which would include a portion of the narrow (<9 meV) $2s2p(^3P^\circ)$ state. It is then impossible to obtain a good fit (i.e., very small probability of less than 0.1%). Inclusion of a second (integrated Fano) profile in this extended region provides a good fit to the data (see Table I(b)]. Not only are the parameters for the large resonance very close to the first fit, but the parameters for the second profile are those that one expects from independent (spectroscopic) evidence.[5–7] This good agreement with known parameters of the neutral state is certainly not a coincidence and can only be interpreted as a confirmation that the assumed nature of the two profiles (i.e., a Fano and an integrated Fano) is basically correct.

TABLE III. A comparison of some of the experimental results for the helium $2s2p^2\,^2D$ negative-ion resonance energy (structure A).

Energy (eV)	Source (experimental)
58.2±0.1	Simpson, Mielczarek, and Cooper[a]
58.2±0.1	Kuyatt, Simpson, and Mielczarek[b]
58.31±0.08	Grissom, Compton, and Garrett[c]
58.23±0.04	Quéméner, Paquet, and Marmet[d]
58.25±0.05	Sanche and Schultz[e]
58.283±0.003	This work

[a]Reference 9.
[b]Reference 10.
[c]Reference 11.
[d]Reference 12.
[e]Reference 13.

B. The $2p^3$ profiles (structures C and D)

A good fit to the whole spectrum shown in Fig. 2 requires *four* profiles to be used. The B profile (i.e., the one obtained from the fit and not apparent from a simple visual inspection of the spectra) has $E_R = 58.309 \pm .003$ eV corresponding to the neutral state $2s2p(^3P^\circ)$. However, the types of profile required for the two new structures are not obvious from our data taken by itself. Although the best fit is obtained using profiles corresponding to negative-ion resonances, using any combination of profiles works almost as well. The signal-to-noise ratio for the two (new) structures is too small to distinguish between the filtered profiles given the large number of parameters (16) required. However, since there are no other neutral helium states in this energy range, the structures cannot be integrated Fano profiles. Therefore, either the structures are negative-ion resonances, or they are due to PCI effects and/or shape resonances.

The question then becomes whether the expected electron affinities of the nearest (higher-lying) neutral states are large enough to assign the new structures to negative-ion states. The next (higher) neutral state is the $2p^2(^3P)$ at 59.674 eV. This electronic configuration is exactly identical to the ground state of carbon $1s^22s^22p^2(^3P)$. Not only do both have the same valence configuration [i.e., $2p^2(^3P)$], but both have spherically

symmetric cores with a net charge of $+2e$. Therefore one would expect their electron affinities to be almost the same.

The measured electron affinity for carbon is 1.268 eV (Ref. 8). The observed E_R for the C structure in our helium spectrum is 58.415±0.005 eV; an energy difference of 1.259 eV from the $2p^2(^3P)$ state. Thus the simplest explanation of these two new structures is that they are $2p^3$ negative-ion resonances. It has been our experience that only one negative-ion structure is observed for each neutral (parent) term and that the negative-ion states observed in the electron-ionization curve usually correspond to the lowest term of the configuration. Thus, by comparison with the homologous carbon states, we can assign the C structure to the $2p^2(^3P)2p(^4S^\circ)$ state. Similarly, we expect that the D structure ($E_R = 58.48 \pm 0.02$ eV) corresponds to the $2p^2(^1D)2p(^2D^\circ)$ state, 1.42±0.02 eV below its parent state. However, this latter assignment is not quite as convincing since the electron affinity for the homologous carbon state is not known.

The four-profile fits give about the same results for the A and B structures as in Table I. The results of our analysis of the spectra are summarized in Table II and a comparison of our E_R value for the A structure with other experimental results is provided in Table III. The best agreement with a theoretical calculation is that of Smith and Golden *et al.*,[14] who found the ^2D state to lie at 58.34 eV, 20 meV below the $2s2p(^3P^\circ)$ state at 58.36 eV. We find the state to be 29±3 meV below the accepted $^3P^\circ$ energy.

*Present address: Division of Health and Science, Red Deer College, Box 5005, Red Deer, Alberta, Canada T4N 5H5.

[1]M. Proulx, P. Marmet, and R. Dutil, Rev. Sci. Instrum. **53**, 778 (1982).
[2]U. Fano, Phys. Rev. **124**, 1866 (1961).
[3]E. Bolduc and P. Marmet, Can. J. Phys. **51**, 2108 (1973).
[4]P. J. M. van der Burgt, J. van Eck, and H. G. M. Heideman, J. Phys. B **19**, 2015 (1986).
[5]W. C. Martin, J. Phys. Chem. Ref. Data **2**, 257 (1973).
[6]G. H. Berry, J. Besesquelles, and M. Dufay, Phys. Rev. A **6**, 600 (1972).
[7]H. Cederquist, M. Kisielinski, and S. Mannervik, J. Phys. B **16**, L479 (1983).
[8]D. Feldman, Chem. Phys. Lett. **47**, 338 (1977).
[9]J. A. Simpson, S. R. Mielczarek, and J. Cooper, J. Opt. Soc. Am. **54**, 269 (1964).
[10]C. E. Kuyatt, J. A. Simpson, and S. R. Mielczarek, Phys. Rev. **138A**, 385 (1965).
[11]J. T. Grissom, R. N. Compton, and W. R. Garrett, Phys. Lett. **30A**, 117 (1969).
[12]J. J. Quéméner, C. Paquet, and P. Marmet, Phys. Rev. A **4**, 494 (1971).
[13]L. Sanche and G. J. Schulz, Phys. Rev. **136**, 1672 (1972).
[14]K. Smith *et al.*, Phys. Rev. A **8**, 3001 (1973).